

Activated molecular adsorption of CO on the Be(0001) surface: A density-functional theory studyShuang-Xi Wang,^{1,2} Yu Yang,² Bo Sun,² Rong-Wu Li,¹ Shao-Jun Liu,¹ and Ping Zhang^{2,*}¹*Department of Physics, Beijing Normal University, Beijing 100875, People's Republic of China*²*LCP, Institute of Applied Physics and Computational Mathematics, P.O. Box 8009, Beijing 100088, People's Republic of China*

(Received 29 May 2009; revised manuscript received 25 August 2009; published 28 September 2009)

Using first-principles calculations, we systematically study the adsorption behavior of molecular CO on the Be(0001) surface. By calculating the potential-energy surfaces, we find that the molecular adsorption of CO on Be(0001) encounters small energy barriers in various entrance channels. The most stable adsorption state is found to be the one at the surface fcc hollow site and the one at the surface top site is the adsorption state that has the smallest energy barrier. Based on electronic structure analysis, we further reveal that during the molecular adsorption, the 5σ bonding and 2π antibonding orbitals of CO hybridize with s and p_z electronic states of Be, causing electrons to transfer from CO to Be.

DOI: 10.1103/PhysRevB.80.115434

PACS number(s): 68.43.Bc, 82.20.Kh, 82.45.Jn, 34.80.Ht

I. INTRODUCTION

It has been of great interest to study the adsorption and dissociation of the diatomic molecule CO on metal surfaces.^{1,2} The essential reason is that the interaction of CO with metal surfaces plays a major role in understanding many phenomena such as heterogeneous catalysis,³ corrosion,^{4,5} gas sensing,⁶ and exhaust gas removing.⁷ For the adsorption on transition-metal surfaces, it has been found that CO molecularly adsorbs on almost all transition-metal surfaces without any energy barriers.^{8,9} In comparison with the vast studies on the adsorption properties of CO on transition metals, the adsorption of CO on simple metal surfaces has seldom been studied yet because of their irrelevance to heterogeneous catalysis. Only very recently, Hellman *et al.* predicted by using first-principles calculations that CO adsorbs on the Al(111) surface molecularly with a small energy barrier,⁹ different from the adsorption behaviors of CO on transition-metal surfaces.

However, many studies are now being applied to explore the possibilities to use fabricated simple metal structures instead of transition metals in catalytical processes¹⁰ because specially fabricated metal structures have displayed quite different catalytic properties with bulk metal materials¹¹ and simple metals are always lighter and cheaper than transition metals. So the adsorption properties of CO on simple metals also need to be studied, especially considering that so scarce theoretical studies of this issue are available in literature and it is impossible for one to give any concluding remarks on the common nature of the CO adsorption on simple sp metal surfaces. Motivated by this observation, in this paper we use first-principles calculations to systematically study the adsorption of CO on the Be(0001) surface. The reason why we choose Be as the prototype for simple metals is that Be has long been used in nuclear reactors as air cleaners to adsorb many kinds of residue gases,¹²⁻¹⁴ and Be is the second lightest metal. Besides and prominently, differing from the bulk, Be surfaces have a large directional s and p electronic distributions around the Fermi energy¹⁵ and thus may display unique interaction with diatomic molecules.¹⁶

By calculating the adiabatic potential-energy surfaces and analyzing the projected density of states (PDOS), we obtain

the adsorption properties of CO on the Be(0001) surface. It is found that CO adsorbs on the Be surface molecularly with small energy barriers. The adsorption interactions are mainly contributed by electrons transfer from bonding orbitals of CO to s and p_z electronic states of Be(0001) surface layer as well as by strong electronic hybridization between antibonding orbital of CO and p_x states of Be.

II. CALCULATION METHOD

Our calculations were performed within density-functional theory using the Vienna *ab initio* simulation package (VASP).¹⁷ The PW91 (Ref. 18) generalized gradient approximation and the projector-augmented wave potential¹⁹ were employed to describe the exchange-correlation energy and the electron-ion interaction, respectively. The cutoff energy for the plane-wave expansion was set to 520 eV. The Be(0001) surface was modeled by a slab composing of five atomic layers and a vacuum region of 20 Å. A comparison showed that the relaxed structure of this slab is similar to our previously used more thick slab that nine atomic layers were included.¹⁶ Thus, it was expected that the present choice of a five-layer slab is reliable and accurate enough for obtaining the essential adsorption and dissociation behavior of CO. A 2×2 supercell, in which each monolayer contains four Be atoms was adopted in the study of the CO adsorption. Our test calculations have showed that a 2×2 supercell is sufficiently large to avoid the interaction between adjacent CO molecules. In fact, by using a more large 3×3 supercell, we have found no essential difference in molecular adsorption energy and adsorbed surface electronic structure from the use of a 2×2 supercell. Integration over the Brillouin zone was done using the Monkhorst-Pack scheme²⁰ with $11 \times 11 \times 1$ grid points. And a Fermi broadening²¹ of 0.1 eV was chosen to smear the occupation of the bands around the Fermi energy (E_F) by a finite- T Fermi function and extrapolating to $T=0$ K. The calculation of the potential-energy surface was interpolated to 121 points with different bond length (d_{CO}) and height (h) of CO at each surface site. The calculated lattice constant of bulk Be (a, c) and the bond length of a free CO molecule are 2.26 Å, 3.58 Å, and 1.14 Å, respec-

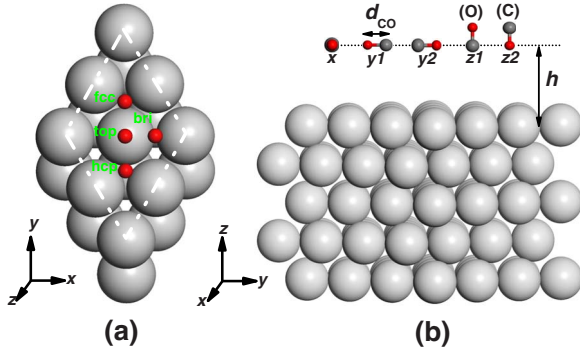


FIG. 1. (Color online) (a) The $p(2 \times 2)$ surface cell of Be(0001) and four on-surface adsorption sites. Here only the outmost two layers of the surface are shown. (b) The sketch map showing that the molecule (with vertical or parallel orientation) is initially away from the surface with a height h . Black, red, and gray balls, respectively, represent for C, O, and Be atoms.

tively, in good agreement with the experimental values of 2.29 Å, 3.588 Å,²² and 1.13 Å.²³

III. RESULTS AND DISCUSSION

First, we do a geometry optimization for the clean Be(0001) surface, during which the bottom two atomic layers of the Be surface is fixed and other Be atoms are free to relax until the forces on them are less than 0.02 eV/Å along the x , y , and z directions (as shown in Fig. 1). Then we calculate a series of two-dimensional (2D) PES cuts for a CO molecule on the relaxed Be(0001) surface. As depicted in Fig. 1, there are four high-symmetry sites on the Be(0001) surface, respectively, the top, bridge (bri), hcp, and fcc hollow sites. Different from the studies on the adsorption of symmetrical diatomic molecules,²⁴ a CO molecule at each surface site has five different high-symmetry orientations. And we here use $y1$ and $y2$, and $z1$ and $z2$ to differentiate C end-on and O end-on orientations. As shown in Fig. 1, there are in total 20 different adsorption channels for CO molecule on the Be(0001) surface. By employing the notations in Fig. 1, we will represent the channels as top- $x, y1, y2, z1, z2$, bri $x, y1, y2, z1, z2$, hcp $x, y1, y2, z1, z2$, and fcc $x, y1, y2, z1, z2$.

The calculated 2D PES cuts along the top- $z1$, top- $z2$, and top- x channels are shown in Figs. 2(a)–2(c), respectively, which are quite different from each other. The calculated 2D PES cuts along other adsorption channels at the top site have similar shapes with that along the top- x channel and thus are not plotted here for brevity. As shown in Fig. 2, we find that the adsorption of molecular CO at the surface top site only occurs when the CO molecule is perpendicular to the metal surface with C end-on orientation. Similar results have been obtained in the CO/Al(111) system.^{8,9} In the following discussion the adsorption state for molecular CO along the top- $z1$ channel will be called as the TZ state. In the PES cut along the top- $z2$ channel, no CO molecular adsorption states exist, and the energy needed to separate the C and O atoms by 1.80 Å is very high (~ 6.8 eV). For the adsorption process along the top- x channel and all similar (namely, top- $y1$ and top- $y2$) channels, there are no adsorption states either.

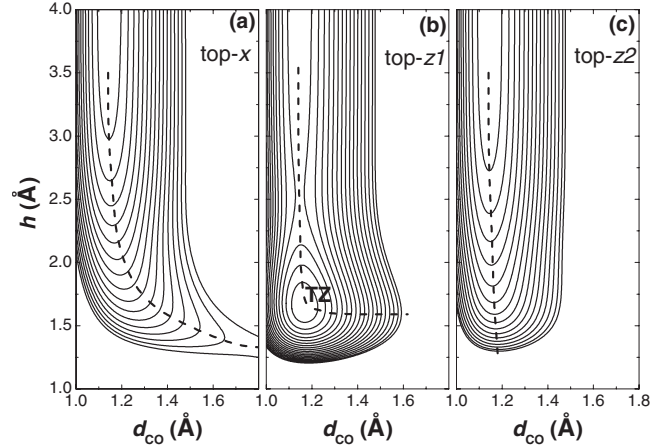


FIG. 2. The 2D PES cuts for the adsorption of CO along the (a) top- x , (b) $z1$, and (c) $z2$ channels. Here, the dashed lines denote the minimum-energy paths and the energy intervals of contours are all 0.20 eV.

However, the energy needed to separate the C and O atoms by 1.8 Å is relatively small (~ 3.05 eV). More interestingly, we find that for a CO molecule to reach the TZ state, it needs to overcome an energy barrier of 0.11 eV, which is quite different from the molecular adsorption of CO on transition-metal surfaces, where the energy barrier is zero.

Through systematic PES calculations, we find that there are always molecular adsorption states when the CO molecule is perpendicular to the Be(0001) surface with C end-on orientations. For illustration the PES cuts along the hcp-, fcc-, and bri- $z1$ channels are shown in Figs. 3(a)–3(c), with the corresponding molecular adsorption states named as the HZ, FZ, and BZ states, respectively. Figure 3(d) summarizes the four minimum-energy paths for the molecular adsorption of CO along the top-, hcp-, fcc-, and bri- $z1$ channels. The corresponding energy barriers for the transition to the molecular adsorption states along these four paths are, respectively, 0.11, 0.32, 0.30, and 0.28 eV. Thus, on one hand it clearly shows that the energy barrier is the smallest for CO to evolve into the TZ state. On the other hand, the energy barriers for these four molecularly adsorbed states are all relatively small, indicating that in experiment they should all be observed at room temperature.

In addition to the four molecularly adsorbed states revealed in Fig. 3(d), we also find another kind of local-minimum states, which is along the bri- $y1$ and $-y2$ channels. Figure 4 and its inset, respectively, show the PES cut along the bri- $y1$ channel and the corresponding minimum-energy path (the situation for the bri- $y2$ channel is quite similar and so is not shown here). However, one can see that the energy barrier to evolve into this local-minimum state (named as LM1) is as large as 1.35 eV. Moreover, the total energy of the LM1 state is 0.80 eV higher than that in the free case (namely, clean Be surface plus isolated CO molecule), indicating that this kind of molecularly adsorbed state seldom happen in practice.

Now let us see the stability of these molecularly adsorbed states by calculating their adsorption energies as follows:

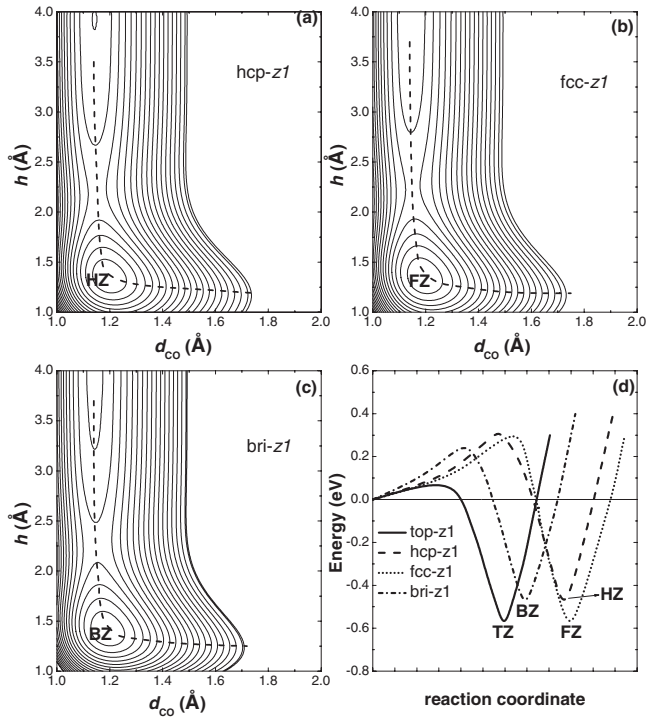


FIG. 3. The 2D PES cuts for the adsorption of CO along the (a) hcp-z1, (b) fcc-z1, and (c) bri-z1 channels. The minimum-energy adsorption paths along the top-, hcp-, fcc-, and bri-z1 channels are summarized in (d).

$$E_{ad} = E_{CO} + E_{Be(0001)} - E_{CO/Be(0001)}, \quad (1)$$

where E_{CO} , $E_{Be(0001)}$, and $E_{CO/Be(0001)}$ are the total energies of the CO molecule, the clean Be surface, and the adsorption system, respectively. According to this definition, a positive value of E_{ad} indicates that the adsorption is exothermic (stable) with respect to a free CO molecule and a negative value indicates endothermic (unstable) reaction. The calcu-

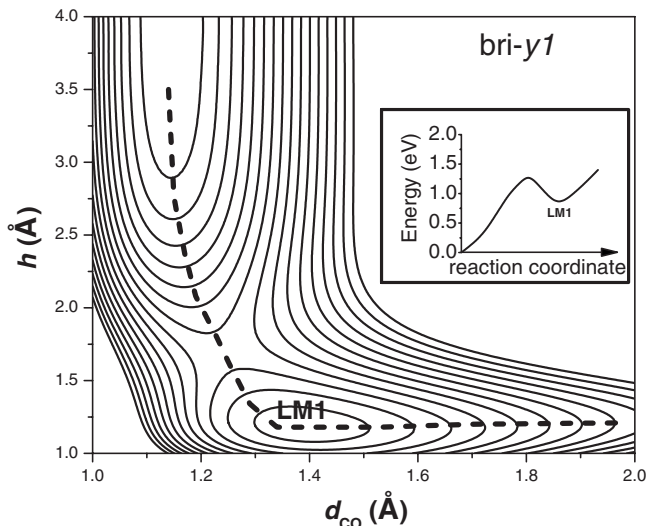


FIG. 4. The 2D PES cut for the adsorption of CO along the bri-y1 channel with the energy interval of 0.20 eV. The inset shows the minimum-energy path along this channel.

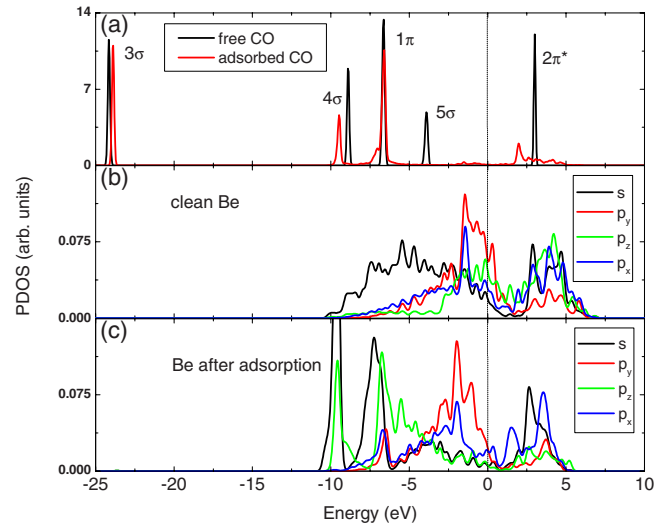


FIG. 5. (Color online) (a) PDOS for the CO molecule before and after the adsorption. [(b) and (c)] PDOS for a surface Be atom before and after the adsorption. The Fermi energy is set to zero.

lated adsorption energies are 0.64, 0.61, 0.68, and 0.51 eV for the TZ, HZ, FZ, and BZ states, and -0.80 and -0.91 eV for the two local-minimum states along the bri-y1 and y2 channels, respectively. From the calculated adsorption energies, we can see that the FZ state is a little more stable than the TZ, HZ and BZ states. In consideration of our previous result that there are less electrons distributed at the surface fcc hollow site than at other sites,²⁵ the relative stability for the four adsorption states seems to indicate that the interactions between the CO molecule and the Be(0001) surface are dominated by charge transfer from CO to Be, which will be discussed in the follows.

As mentioned above, the energy differences among the TZ, HZ, FZ, and BZ states are very tiny, and the energy barriers to reach them are also small enough to be overcome at room temperatures. So for further illustration, we here calculate the PDOS for all of these molecularly adsorbed states. We find that the four adsorption states have similar PDOS characters. As a typical example, we plot in Fig. 5 the PDOS for the CO molecule and one surface Be atom in the TZ state. For comparison, the PDOS for the free CO molecule and clean Be(0001) surface are also shown in Fig. 5. One can clearly see from Fig. 5(a) that after adsorption, the 3σ bonding orbital of the CO molecule negligibly changes, while the 4σ and 1π bonding orbitals change a little by losing few electrons, and the 5σ bonding and 2π antibonding orbitals almost disappear. So during the molecule-metal interaction, the electrons in the 5σ bonding orbital of CO all transfer to the electronic states of Be(0001) surface. Besides, we see that no charge transfer from electronic states of Be back to the CO molecule as there are no new orbital occupation in the PDOS of CO after adsorption. So the net charge transfer during the adsorption is from CO to Be. This result confirms our earlier speculation that the FZ state is stabler than the TZ, HZ, and BZ states because electrons are easier to transfer from CO to Be at the surface fcc site. Moreover, since the 5σ bonding orbital of CO is asymmetric in that more electrons distribute around C than around O atom,²⁶ the

present PDOS analysis can also explain why only along the channels with C end-on orientations there are molecularly adsorbed states. The reason is that charge transfer happens easier when C atoms are close enough to the Be surface.

From Figs. 5(b) and 5(c) one can see that the s and p_z electronic states of surface Be shift to lower energies during adsorption process, indicating that they accept electrons from bonding molecular orbitals of CO. In addition, there are two new peaks for Be s and p_z states, aligning in energy with CO 4σ and 1π orbitals, respectively, indicating as well an observable covalency among these orbitals. Another fact is that at the energy range above the Fermi energy, the s and p_z electronic states of Be also change a lot by hybridizing with the 2π antibonding orbital of CO. In total, the electronic states of Be that interact with molecular orbitals of CO are mainly the s and p_z states. And correspondingly, one can see from Figs. 5(b) and 5(c) that the Be p_x/p_y states change very little during the molecular adsorption of CO.

To gain more insight into the nature of chemical bonding between CO and Be during surface adsorption, we also analyze the difference electron density $\Delta\rho(\mathbf{r})$ for the four stable molecularly adsorbed states. Here $\Delta\rho(\mathbf{r})$ is obtained by subtracting the electron densities of noninteracting component systems, $\rho^{\text{Be}(0001)}(\mathbf{r}) + \rho^{\text{CO}}(\mathbf{r})$, from the density $\rho(\mathbf{r})$ of the CO/Be(0001) system, while retaining the atomic positions of the component systems at the same location as in CO/Be(0001). As a typical example, the calculated $\Delta\rho(\mathbf{r})$ for the TZ state is shown in Fig. 6. We can see that there is a large charge-depletion area between the C and O atoms, showing the depopulation of the 5σ bonding orbital of CO by transferring electrons out. And correspondingly, there is a large charge accumulation near the Be(0001) surface, indicating acceptance of electrons of the s and p_z electronic states of the surface Be atoms. Remarkably, this charge accumulation is highly directional instead of isotropically itinerant around the surface. In this aspect, the acceptance of electron makes the Be(0001) surface rather insulating than metallic. The same conclusion can also be derived from Fig. 5, which shows that the surface Be PDOS at the Fermi energy is largely decreased after molecular adsorption of CO.

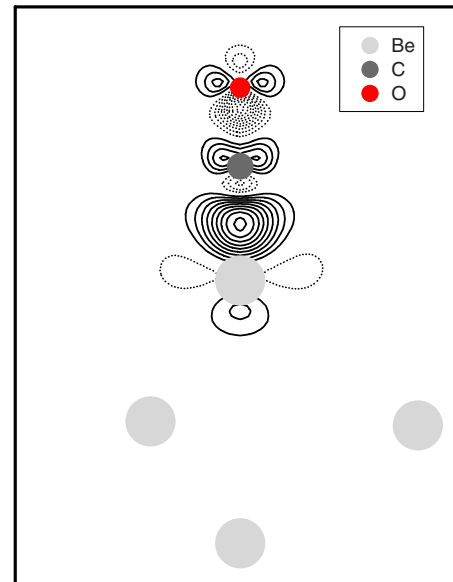


FIG. 6. (Color online) Difference electron density for the most stable TZ adsorption state of CO on the Be(0001) surface. Black, red, and gray balls denote C, O, and Be atoms, respectively. Solid and dotted lines represent charge accumulation and depletion, respectively.

IV. CONCLUSION

In conclusion, we have studied the adsorption behavior of CO on the Be(0001) surface by using first-principles DFT method. Through systematic PES calculations, we have revealed that the adsorption of CO on the Be(0001) surface is molecular with small energy barriers. The stable adsorption states all have C end-on orientations. The most stable adsorption state for molecular CO has been found to be along the fcc- $z1$ channel while the adsorption state with the smallest energy barrier is along the top- $z1$ channel. It has also been shown that the interactions between CO and the Be surface are dominated by charge transfer from CO to Be. We expect that the present results are greatly helpful for the practical usage of Be surfaces in adsorbing residual gases in experimental nuclear fusion reactors.

*Corresponding author; zhang_ping@iapcm.ac.cn

¹G. R. Darling and S. Holloway, *Rep. Prog. Phys.* **58**, 1595 (1995).

²D. A. King and D. P. Woodruff, *The Chemical Physics of Solid Surfaces and Heterogeneous Catalysis* (Elsevier, Amsterdam, 1988).

³A. Nilsson and L. G. M. Pettersson, *Surf. Sci. Rep.* **55**, 49 (2004).

⁴K. E. Heusler and G. H. Cartledge, *J. Electrochem. Soc.* **108**, 732 (1961).

⁵P. Marcus, *Corrosion Mechanisms in Theory and Practice* (Marcel Dekker, New York, 2002).

⁶B. Srinivasan and S. D. Gardner, *Surf. Interface Anal.* **26**, 1035

(1998).

⁷J. Libuda and H. J. Freund, *Surf. Sci. Rep.* **57**, 157 (2005).

⁸B. Hammer, Y. Morikawa, and J. K. Nørskov, *Phys. Rev. Lett.* **76**, 2141 (1996).

⁹A. Hellman, B. Razaznejad, and B. I. Lundqvist, *Phys. Rev. B* **71**, 205424 (2005).

¹⁰X. C. Ma, P. Jiang, Y. Qi, J. F. Jia, Y. Yang, W. H. Duan, W. X. Li, X. H. Bao, S. B. Zhang, and Q. K. Xue, *Proc. Natl. Acad. Sci. U.S.A.* **104**, 9204 (2007).

¹¹M. S. Chen and D. W. Goodman, *Science* **306**, 252 (2004).

¹²S. Zalkind, M. Polak, and N. Shamir, *Surf. Sci.* **385**, 318 (1997).

¹³F. Scaffidi-Argentina, G. R. Longhurst, V. Shestakov, and H. Kawamura, *J. Nucl. Mater.* **283-287**, 43 (2000).

- ¹⁴S. Zalkind, M. Polak, and N. Shamir, *Surf. Sci.* **513**, 501 (2002).
- ¹⁵J. C. Boettger and S. B. Trickey, *Phys. Rev. B* **34**, 3604 (1986).
- ¹⁶P. Zhang, B. Sun, and Y. Yang, *Phys. Rev. B* **79**, 165416 (2009).
- ¹⁷G. Kresse and J. Furthmuller, *Phys. Rev. B* **54**, 11169 (1996).
- ¹⁸J. P. Perdew and Y. Wang, *Phys. Rev. B* **45**, 13244 (1992).
- ¹⁹G. Kresse and D. Joubert, *Phys. Rev. B* **59**, 1758 (1999).
- ²⁰H. J. Monkhorst and J. D. Pack, *Phys. Rev. B* **13**, 5188 (1976).
- ²¹M. Weinert and J. W. Davenport, *Phys. Rev. B* **45**, 13709 (1992).
- ²²E. Wachowicz and A. Kiejna, *J. Phys.: Condens. Matter* **13**, 10767 (2001).
- ²³K. P. Huber and G. Herzberg, *Constants of Diatomic Molecules* (Van Nostrand, New York, 1979).
- ²⁴Y. Yang, G. Zhou, J. Wu, W. H. Duan, Q. K. Xue, B. L. Gu, P. Jiang, X. C. Ma, and S. B. Zhang, *J. Chem. Phys.* **128**, 164705 (2008).
- ²⁵S. X. Wang, Y. Yang, B. Sun, R. W. Li, S.-J. Liu, and P. Zhang, (unpublished).
- ²⁶A. Föhlisch, M. Nyberg, J. Hasselström, O. Karis, L. G. M. Pettersson, and A. Nilsson, *Phys. Rev. Lett.* **85**, 3309 (2000).